Assembly and aiming of bacterial Type VI secretion systems

Jing Wang[1*], Maj Brodmann[1*], Marek Basler[1]

[*] contributed equally

[1] Biozentrum, University of Basel, Klingelbergstrasse 50/70, CH - 4056 Basel, Switzerland

Abstract:

Bacteria need to deliver large molecules out of the cytosol to the extracellular space or even across membranes of neighboring cells to influence their environment, prevent predation, defeat competitors or to communicate. A variety of protein secretion systems have evolved to make this process highly regulated and efficient. The Type 6 secretion system (T6SS) is one of the largest dynamic assemblies in Gram-negative bacteria and allows for delivery of toxins into both bacterial and eukaryotic cells. The recent progress in structural biology and live-cell imaging of T6SS shows that a long contractile sheath assembles from a cell envelope-anchored baseplate and membrane complex around a rigid tube with associated toxins. Rapid sheath contraction releases large amount of energy to push the tube and toxins through the membranes of neighboring target cells. To increase efficiency of toxin translocation, some bacteria dynamically regulate subcellular localization of T6SS to precisely aim at their targets.

1.T6SS mode of action

The bacterial Type 6 secretion system (T6SS) shares evolutionary origin with contractile phage tails and other extracellular contractile protein translocation nanomachines such as R-type pyocins (8, 44, 66). T6SS apparatus is composed of 13 core proteins, with a set of regulatory and accessory proteins for specialized functions (10). The whole T6SS was visualized in bacteria by cryo-electron tomography (7, 19), which shows that T6SS is tethered to the cell envelope by a membrane complex (28), which is a platform for assembly of a phage-like baseplate with a central spike and effectors (22, 59). Baseplate assembly initiates copolymerization of a contractile sheath around a rigid inner tube (88, 89). Upon unknown signal, the long spring-like sheath quickly contracts progressively from the baseplate to the distal end and physically pushes the inner tube and spike with effectors out of the cell and through a membrane of a neighboring cell (42, 89) (Figure 1, Movie 1).

An important advantage of the T6SS mode of action is that the sheath contraction releases large amount of energy that can be used to penetrate physical barriers. Single sheath contraction, which happens in less than 2 ms (88), could release the same amount of energy as the conversion of one thousand molecules of ATP to ADP (89). This allows T6SS to deliver large hydrophilic effectors even across two membranes and the peptidoglycan layer of Gram-negative bacterial cells (87). However, the T6SS mode of action also has significant drawbacks. Most T6SS substrates are secreted by binding to the spike components and thus with every firing of T6SS only a few copies of the cargo proteins are secreted (23, 65, 81). In addition, even the most active bacteria fire T6SS only approximately once per minute (6, 7, 13, 28, 35, 61, 70, 77). The extended sheath is assembled around the inner tube, which is mostly lost upon firing and has to be resynthesized (89). Furthermore, the contracted sheath cannot be directly used for a new assembly and the sheath subunits have to be unfolded by a

dedicated ATPase (ClpV) (6, 9). Finally, since T6SS substrates are directly pushed across the target membrane by the tube, the T6SS has a limited reach and proteins can be delivered only if the target cell is in a close proximity and the T6SS fires in the right direction (37, 87).

Here, we review recent insights into the structure and assembly of T6SS and the mechanisms that evolved in certain bacteria to dynamically localize T6SS to minimize costs and increase efficiency of toxin translocation and target cell killing.

2.T6SS structure and assembly

2.1. Membrane complex

The membrane complex is composed of three proteins, TssJ, TssL and TssM. TssJ is a lipoprotein anchored to the outer membrane (OM) by N-terminal cysteine acylation (3). The protein itself is confined within the periplasm and folds as a β-sandwich resembling transthyretin with an additional helical domain and a protruding loop (L1-2 loop) (30, 68, 71) (Figure 2a). The helical domain stabilizes TssJ and the L1-2 loop interacts with TssM (30). TssJ is required for assembly of the other membrane complex components TssJ and TssM (28), however, the high-order assembly of TssJ seems to be driven by TssM (Figure 2b, 2c) (69).

TssM was early identified as a T4SS IcmF-like protein (4, 17, 52). The N-terminus of TssM is a large cytosolic domain with NTPase activity flanked by 3 trans-membrane helices (53) (Figure 2d). The C-terminal domain traverse the entire periplasm and reaches OM by contacting TssJ (28). This periplasmic domain has an OmpA-like peptidoglycan binding motif and oligomerizes as the core of the membrane complex (4, 69, 93). Density corresponding to the OmpA-like domain is missing in the membrane complex *in situ* cryo-ET structure, indicating that it is rather flexible compared to the rest of the membrane complex. The very C-terminus of TssM is exposed on the cell surface and part of the TssM β-stranded domain can

breach the OM transiently during T6SS firing (28). In the recent membrane complex structure, TssM C-terminal extremity folds within the periplasm domain as an α-helix that connects to the rest of the TssM by a 20 amino acid long linker. TssM C-terminus may extend outside of the cell in the native state and be thus responsible for sensing environmental clues to activate T6SS assembly.

TssL is an inner membrane (IM) protein homologous to T4bSS associated IcmH/DotU (29). Its function requires dimerization controlled mainly by the N-terminal trans-membrane segment. Mutations in TssL abolished TssL function (Figure 2e) (29), as these loops and cleft are necessary for TssL interactions with baseplate as well as membrane complex (97). The baseplate binding loops are not conserved among the TssL proteins and may determine specificity during T6SS assembly in the organisms encoding several T6SS (29).

Overexpression of *E. coli* (EAEC) TssJ, TssM and TssL allowed *in-situ* visualization of the membrane complex by cryo-ET (Figure 2f). A "Y-shaped" core of membrane complex spanning the periplasm is flanked by a cap embedded in the outer membrane and a base embedded in the inner membrane (IM) (69). Interestingly, cryo-ET and single particle analysis of the EAEC T6SS membrane complex revealed a 5-fold symmetry structure. This is in contrast to the rest of the T6SS apparatus, which follows a C6 symmetry (except C3 for VgrG and C1 for PAAR). Therefore, this symmetry mismatch will have to be resolved between TssL/M and the binding partners in the baseplate TssK. This would maybe require more flexible binding sites and could explain why the cytoplasmic part of the complex shows heterogeneous density that fails to yield any consensus structure upon averaging. Alternatively, proper assembly of the membrane complex with C6 symmetry might require a scaffold protein or chaperon-like activity of other T6SS components, which were absent in the *E. coli* strain over-expressing TssJLM (69, 93).

This structure of membrane complex is likely in a "closed" conformation, since the periplasm channel is constricted by a TssM loop protruding into the central lumen (Figure 2c) (69, 93). This constriction is displaced either by TssM conformational change triggered by movement in baseplate during initiation of sheath contraction or it can simply be forced open during tube/spike secretion through the membrane complex.

2.2. Baseplate structure

Similarly to the baseplates of contractile phages, the T6SS baseplate comprises a central hub surrounded by 6 wedges (Figure 3a). It initiates the assembly of the Hcp tube and sheath in an extended high-energy state, and change in baseplate structure is likely required for triggering sheath contraction (22, 45, 59, 62). The central hub is made of a trimeric VgrG, which connects the wedges and initiates Hcp tube assembly. The base of the VgrG structure has a similar fold as an Hcp dimer. Therefore, VgrG trimer with a pseudohexameric structure provides a platform to seed Hcp polymerization. Several unstructured loops of Hcp hexamer absent from x-ray structures become ordered in Hcp tube (89). These unstructured regions could be preventing Hcp stacking but may readily fold and initiate polymerization when initiator complex is bound (VgrG, TssE and sheath). The needle domain of T6SS VgrG lacks a sharp point for membrane piercing (83), however, this blunt end binds a small protein with a characteristic proline–alanine–alanine–arginine (PAAR) domain sequence. VgrG/PAAR complex then serves as a docking structure for many effectors that may require help of chaperons to assemble (67). Diversity of effectors and their functions were reviewed elsewhere (1, 47).

The wedge of T6SS contains TssE-TssF-TssG-TssK at 1:2:1:6 stoichiometry (Figure 3b) (22, 62). TssE is a universally conserved gp25-like protein in contractile injection systems (45) resembling the handshake domain of TssB-TssC and was suggested to play an important role

121 in the initiation of sheath assembly to the extended state. Somewhat surprisingly, *tssE*-
122 negative strain of *V. cholerae* assembles functional T6SS albeit at a much lower frequency
123 (87). Whether another protein can complement the absence of TssE is unknown.

124 TssF folds as a three-domain wing-like structure (22, 62). Two TssF molecules within a single
125 wedge interacts with the conserved EPR motif of TssE (84) and TssG (22, 62). TssG has a
126 fold similar to TssF, except lacking the large TssF central wing-like domain. TssG also
127 features two TssK binding loops that are absent in the TssF (Figure 3b). The C-terminal fold
128 of TssG can be superimposed with TssF C-terminal domain, suggesting that these proteins
129 evolved from a common ancestor by gene duplication (62). $(TssF)_2$-TssG heterotrimer is
130 tightly interdigitated. Their N-terminal domains form 3-helix bundle resembling the "core
131 bundle" of phage T4 and their C-terminal domains form a triangular core resembling the T4
132 'trifurcation unit" (62, 84) (Figure 3b).

133 In phage T4, a LysM domain containing protein gp53 functions as inter-wedge clamp that
134 joints the wedges into the baseplate (2). T6SS lacks gp53 orthologs maybe to allow quick
135 baseplate disassembly upon sheath contraction. It is unclear what triggers and stabilizes the
136 assembly of 6 wedges around the central hub. It could be interaction with the membrane
137 complex or in some cases be even facilitated by additional proteins such as TssA1 of *P.*
138 *aeruginosa* (64).

139 Unlike other T6SS baseplate components, which share common evolutionary origin with
140 contractile phages (11, 59), TssK is clearly a homolog of the receptor binding protein (RBP)
141 from non-contractile phages (60). The main difference between TssK and phage RBP lies in
142 the C-terminal head domain that recognizes the binding partner. Based on the isolated wedge
143 structure, each wedge complex contains two TssK timers attaching to one of the two extended
144 loops of TssG (Figure 3b). The conserved loops of TssG interact by complementary surfaces
145 with the hydrophobic N-termini of the TssK. Binding of the TssK to TssG is reminiscent of

the attachment observed for RBP to phage baseplates, such as in TP901-1 (86) and P2 (79). TssK plays a central role in T6SS assembly by docking the baseplate to the membrane complex as it interacts directly with cytosolic domains of TssL and TssM (99). The self-association of TssM and TssL as dimer is critical for T6SS function (22, 29, 98), suggesting that matching dimers of TssK and TssL/TssM mediates the baseplate to membrane complex interaction. TssK trimer is mobile relative to $(TssF)_2$-TssG module as revealed by cryo-EM (62). One can envision that TssK detects the mechanical distortion from membrane complex undergoing conformational change and propagates it to downstream baseplate components. The resulting reorganization of baseplate eventually leads to sheath contraction. Alternatively, cytosolic signaling pathways or interactions with other proteins might modulate the affinity of TssK to the membrane complex and thus precisely control the timing of T6SS assembly or contraction.

2.3. Tail-sheath complex

During T6SS assembly, sheath subunits (TssB-TssC) polymerize in a meta-stable, extended state that requires the presence of baseplate and tube (Hcp). Contraction of the sheath provides energy to push and rotate the inner tube out of bacteria cell envelope for effector delivery. Structure of contracted T6SS sheath from several bacteria have been determined by cryoEM (24, 42, 73). Despite sequence variations, the overall structure and the assembly of the T6SS sheath is conserved (Figure 4b, 4d). Each sheath subunit consists of two proteins TssB (VipA) and TssC (VipB), which fold into three domains (Figure 4a). Domains 1 and 2 of the sheath subunit are similar to those of other contractile injection systems and they connect sheath subunits as a meshwork. However, the third α-helical domain inserted into the Domain 2 is T6SS specific. Domain 3 assembles from TssB C-terminus and TssC N-terminus, which includes the ClpV binding site.

To obtain a structure of the extended sheath, a non-contractile sheath was generated by elongating TssB linker that allowed an aberrant wiring of the sheath meshwork and prevented its contraction during purification from cells (12) (Figure 4a, 4c). This non-contractile sheath contains wild type Hcp tube, which is made of stacked Hcp hexamers following the helical symmetry of the extended sheath. The free solvation energy stabilizing Hcp tube is weaker compared to T4 and R-type pyocin (89), which may explain why Hcp tube was never isolated and apparently disassembles after secretion out of cells.

Comparison of the extended T6SS tube–sheath complex with the contracted sheath suggests a mechanism by which sheath contraction is coupled to the translocation of the inner tube. Upon contraction, the sheath expands radially to release the Hcp tube and compresses vertically to push the tube forwards. Difference in the helical parameters of the extended and contracted sheath shows that T6SS functions as a powerful drill. Contraction of a 1 μm long sheath would push the Hcp tube by 420 nm and rotate it by 4.2 turns within a few milliseconds (42, 87, 89).

Importantly, Domain 3 is folded on the surface of the extended sheath making the ClpV binding site on the TssC inaccessible (63, 89) (Figure 4e, 4f). During sheath contraction the Domain 3 is exposed on the surface and becomes unstructured to allow ClpV binding and specific refolding of the contracted sheath (6). ClpV is a hexameric AAA+, which pulls on the exposed N-terminus of TssC and releases it from the contracted sheaths to replenish the pool of sheath subunits for new rounds of assembly. In *F. novicida* (13) where a canonical ClpV is missing, the contracted sheath of T6SS is dissembled by a general purpose unfoldase ClpB. Several recent structures of ClpB have demonstrated a general mechanism by which unfoldase couples sequential ATP hydrolysis to substrate threading during disaggregation (25, 33, 94). Interestingly, in some organisms like *P. aeruginosa*, an additional protein, TagJ, was

shown to interact with both sheath (TssB) and ClpV, however the exact role of TagJ is unclear as its deletion has no clear phenotype (31, 51) (Figure 4b).

2.4. TssA proteins

Proteins possessing a conserved N-terminal ImpA_N region are considered members of the TssA family. The C-terminal sequences of TssA are highly diverse, which further divide members of TssA into two clades (27). The function and localization of each TssA clade varies (27, 64, 100). Both TssA clades seem to stabilize baseplate. In addition, *E. coli* TssA2 was suggested to reinforce 6-fold symmetry to the membrane complex (101) and coordinate copolymerization of sheath and tube (75, 100).

The overall architecture of TssA-assembled complex is represented by *E. coli* TssA2 (100). It consists of a central core bearing six extended arms yielding a snowflake-like structure. Ring-like oligomer of the C-terminal domain (CTD) constitutes the central core. The middle domain (or flexible linker in the case of TssA1) can dimerize and together with the N-terminal domain is composing the extending arms. The conserved N-terminal ImpA_N region folds as a compact anti-parallel α-helix domain that probably performs a common function (27).

Interestingly, a membrane associated TagA protein arrests sheath polymerization and stabilizes the extended sheath (75). TagA also contains N-terminal ImpA-domain and thus the TagA–TssA interaction might be mediated by dimerization of their N-termini (100). Despite the sequence and structural diversity, the C-terminal domain (CTD) of all TssAs investigated to date (TssA1 of *P. aeruginosa* and *B. cenocepacia*, TssA2 from *A. hydrophila* and *E. coli*) are capable of forming ring-like oligomers, which seem to be the structural determinant for TssA self-association (27, 64, 100).

3.Subcellular localization of T6SS assembly

Regulation of T6SS activity mainly involves regulation of expression of the T6SS genes on a transcriptional or posttranscriptional level as a response to diverse environmental stimuli (21, 41, 46, 54). Interestingly, live-cell imaging of TssB or ClpV dynamics showed that bacteria have different T6SS assembly patterns and may dynamically localize the T6SS within the bacterial cell. *V. cholerae* or *A. baylyi* build several T6SS sheaths per cell and fire constantly in apparently random directions (6, 70). Enteroaggregative *E. coli* (EAEC) repeatedly assembles Sci-1 T6SS at one or two apparently random positions within the cell (28). *P. aeruginosa* assembles one of its three T6SS within seconds of an attack from other bacteria at the site of the inflicted damage to quickly retaliate (5). The majority of *S. marcescens* assemble one T6SS sheath at random positions in the cell, however, rely on regulated T6SS assembly for efficient killing of prey cells (35, 61). In addition, intracellular pathogens *F. novicida* and *B. thailandensis* assemble their anti-eukaryotic T6SS on the poles (13, 77).

3.1. Threonine phosphorylation pathway mediates T6SS repositioning

The first example of post-translational regulation of T6SS assembly was described in *P. aeruginosa* by a threonine phosphorylation pathway (TPP) (57). Later, TPPs were shown to regulate initiation and positioning of T6SS assembly in several organisms (5, 32, 48, 61) (Figure 5). TPPs have a sensor module, which senses a signal and activates a kinase (PpkA). An activated kinase then phosphorylates a target protein, which in turn initiates T6SS assembly. Eventually, a phosphatase (PppA) dephosphorylates the target protein and thus prevents further T6SS assembly initiation. *P. aeruginosa* cluster H1-T6SS encodes a complete TPP with a sensor module composed of TagQ/R/S/T, a kinase PpkA, which phosphorylates Fha and a phosphatase PppA. Other species like *S. marcescens* and *A. tumefaciens* possess only PpkA, PppA, Fha. In addition, T6SS assembly in these three organisms is blocked by

TagF and its deactivation can trigger T6SS assembly in a TPP-independent manner (48, 49, 61, 82).

3.1.1. Signal sensing and kinase activation

The sensor module TagQRST in *P. aeruginosa* was shown to be required for sensing T6SS attacks from either sister cells or other bacteria as well as cell envelope stress induced by polymyxin B, Type 4 secretion system, chelation of ions or extracellular DNA (5, 6, 36, 91). Lipoprotein TagQ is anchored to the periplasmic side of the outer membrane by a conserved lipobox and binds periplasmic TagR (16). Interaction of TagR with the periplasmic domain of PpkA may result in activation of its kinase activity (38). This suggests that TagQ could be sequestering TagR to the outer membrane to prevent its binding to PpkA and thus T6SS activation, however, TagQ has likely an additional role since deletion of either TagQ or TagR prevents T6SS assembly (16).

The components TagS and TagT form a putative ABC transporter with a homology to the Lol complex, which transports lipoproteins (58). TagS forms an integral membrane protein with a long periplasmic loop and TagT is an ATPase and contains a Walker A and B motif, which is required to hydrolyze ATP *in vitro* (16). TagS or TagT are required for full T6SS activation (5, 16), however, despite homology to the Lol complex, it is unclear if TagS and TagT transport any substrates. An obvious candidate would be TagQ or TssJ, however deletion of TagS and TagT does not seem to alter their membrane localization (16).

In *S. marcescens*, periplasmic RtkS (regulator of T6SS kinase in *Serratia*) was shown to be required for efficient killing of prey cells but dispensable for T6SS activity in liquid culture. Signals sensed by RtkS are unknown and it is also unclear whether RtkS directly interacts with PpkA, however, deletion of *rtkS* resulted in destabilization and degradation of PpkA (61).

The serine/threonine kinase PpkA is an inner membrane protein with a periplasmic domain and cytosolic kinase domain. PpkA may be activated by interaction with a periplasmic protein (*e.g.* TagR), which results in PpkA dimerization. PpkA dimer auto-phosphorylates and activates T6SS assembly by phosphorylating a T6SS component (32, 38, 49, 56, 57). While kinase domain is conserved, the structure of the periplasmic domain differs between *S. marcescens* and *P. aeruginosa* (32). This is likely because each PpkA responds to a different signal and binds different periplasmic protein.

3.1.2. Activation of T6SS assembly by protein phosphorylation

In both *P. aeruginosa* and *S. marcescens*, activated PpkA phosphorylates Fha, which likely recognizes phosphorylated PpkA via its Forkhead-asscociated (FHA) domain known to bind phosphopeptides (57). However, it is unclear how phosphorylation of Fha promotes T6SS assembly (38, 57, 61). Interestingly, Fha forms foci in *P. aeruginosa* independently of its phosphorylation status (57), however, membrane anchored PpkA is still required for formation of these foci (38). This suggests that PpkA may have an additional structural role in Fha foci formation and T6SS assembly initiation. In *P. aeruginosa*, Fha phosphorylation is increased when cells are incubated on a solid surface suggesting that cell-cell interactions result in PpkA activation (16). This activation could be a consequence of T6SS dueling between sisters cells (6). In contrast, the majority of Fha in *S. marcescens* is phosphorylated also in a liquid culture, where there are minimal or no cell-cell interactions (32).

In *A. tumefaciens*, PpkA phosphorylates membrane complex component TssL leading to a conformational change in TssM (49). TssM is an inner membrane ATPase with Walker A and B motifs and the conformational change triggers ATP hydrolysis. However, TssL-TssM interaction is independent of ATPase activity of TssM (53). Phosphorylated TssL interacts with Fha and the Fha-pTssL complex promotes recruitment of secretion substrates Hcp and

effector Atu4347 to TssL (49). It is unclear how is ATPase activity of TssM involved in recruiting the secreted proteins and if formation of this complex requires additional proteins (49, 53). TssM of *P. aeruginosa*, *V. cholerae* and *Edwardsiella tarda* also contain Walker A and B motifs (53), however ATP hydrolysis does not seem to be important for T6SS activity in *E. tarda* (96).

An interesting case is *V. alginolyticus*, which uses the TPP of its second T6SS cluster to regulate T6SS assembly as well as gene expression. As in *A. tumefaciens*, PpkA phosphorylates TssL, which results in binding of Fha and increase in T6SS activity. In addition, PpkA phosphorylates a non-T6SS substrate VtsR. Phosphorylated VtsR activates LuxO and subsequently promotes expression of T6SS-2 and quorum sensing (92).

3.1.3. T6SS assembly deactivation

In *P. aeruginosa* and *S. marcescens*, phosphatase PppA is responsible for dephosphorylation of Fha and thus shutting down T6SS activity. Since T6SS activity is low in *P. aeruginosa*, deletion of PppA results in an increase of T6SS activity and Hcp secretion (5, 16, 38, 57). However, in *S. marcescens*, deletion of PppA does not increase Hcp secretion in liquid medium, suggesting that the system is already at the maximum activity. Interestingly, in both species, *pppA* deletion strains repeatedly assemble T6SS at the same location within the cells for several rounds of firing (5, 61). This has a major consequence for interaction with competing bacteria, because *P. aeruginosa pppA*-negative strain cannot distinguish between T6SS positive attackers and T6SS negative bystander cells and kills both to a similar extent. Importantly, the killing rate of T6SS positive attackers by *pppA*-negative strain is low, even though *pppA*-negative strain secretes significantly more effectors than the wild-type strain (5, 36). Similar observation was also made for *S. marcescens*, where *pppA*-negative strain kills prey cells poorly despite high T6SS activity (32, 61). This suggests that PppA activity is important to prevent excessive firing of T6SS in one direction and by stopping the assembly

allows T6SS to reposition to a new subcellular location upon sensing a signal, which in turn is required for efficient killing of target cells.

3.2. TPP independent regulation

In addition to TPP, TagF regulates T6SS assembly in *P. aeruginosa* and *S. marcescens* by a poorly understood mechanism. For *P. aeruginosa*, it was shown that TagF sequesters Fha to prevent T6SS assembly (48) and indeed deletion of TagF activates T6SS even in the absence of TagQRST and PpkA (82). Importantly, even strains lacking TPP, like *V. cholerae*, also require Fha for T6SS activity suggesting that Fha is an important scaffold protein for assembly of other T6SS components (95). Similarly to *P. aeruginosa*, when *tagF* is deleted in the *ppkA*-negative strain of *S. marcescens*, T6SS assembly is restored. It is however unclear whether TagF interacts with Fha or other T6SS components.

In *A. tumefaciens*, TagF and PppA are fused into a single polypeptide, however, both independently block T6SS activity (48, 49). TagF domain binds Fha, however, this seems insufficient to prevent T6SS assembly as a TagF-domain mutant, which is still able to bind Fha, loses its ability to repress T6SS activity. This suggests that the TagF domain is also involved in Fha-independent repression (48). Similarly to *S. marcescens*, efficiency of target cell killing is decreased in the absence of PpkA and TagF-PppA even though the overall T6SS activity remains high (48), suggesting that TPP components and TagF are important for sensing prey cells and/or repositioning the T6SS apparatus.

3.3. Regulation of T6SS localization by peptidoglycan cleaving enzymes

Many cell-envelope spanning complexes like flagellum, T3SS or T4SS, require specialized lytic trans-glycosylases for insertion into the peptidoglycan layer (26, 76, 85). Interestingly,

two dedicated peptidoglycan cleaving enzymes were shown to be required for T6SS assembly and thus their control in response to certain signals or stimuli could, in principle, allow for dynamic localization of T6SS assembly. Enteroaggregative *E. coli* (EAEC) requires general lytic trans-glycosylase MltE to insert membrane complexes of the Sci-1-T6SS. Lipoprotein MltE is located at the outer membrane and interacts with the periplasmic domain of TssM. How MltE is activated by TssM and if additional components are required is unknown (74). In *Acinetobacter*, the L,D-endopeptidase TagX is encoded in the T6SS cluster and is required for T6SS activity (70, 90). Since T6SS assembles at low frequency also in *tagX*-negative strain, it is likely that additional mechanisms may allow for assembly initiation or peptidoglycan cleavage and that TagX is only required for integration of the T6SS apparatus into the peptidoglycan layer and not for T6SS function (70).

3.4. Polar localization of T6SS

Polar localization is a potential mechanism for bacteria to coordinate function of multiple protein complexes, such as pili, flagella or secretion systems. Positioning of macromolecular assemblies on the bacterial pole is achieved by several distinct mechanisms, some of which are well understood (43). Strikingly, polar localizations was shown for almost all types of secretion systems most of which are required for host-pathogen interactions (15, 18, 20, 39, 55, 72, 80). In addition, secretion of typhoid toxin from *Salmonella* Typhi requires localized cleavage of peptidoglycan, which is specifically edited on the bacterial pole to contain LD-crosslinks (34). Importantly, polar localization is required for successful effector translocation and progression of infection in *L. pneumophila* (40).

B. thailandensis and *F. novicida* were shown to assemble polarly localized T6SS required for host-pathogen interactions (13, 77). *B. thailandensis* T6SS-5 is required for formation of multinucleated giant cell (77, 78), while *F. novicida* requires the T6SS for phagosomal escape

and assembles one polar T6SS per cell *in vitro* and inside macrophages (13, 14). For the T6SS, sheath length defines the reach of T6SS attack as the sheath contracts to half of its extended length (7). Therefore, polar T6SS assembly may allow assembly of longer sheaths in rod shaped bacteria and thus can increase efficiency of effector delivery. In the case of *F. novicida*, it would be delivery across phagosomal membrane, in case of *B. thailandensis* it would be the ability to induce membrane fusion of neighboring host cells (14, 78). However, polar localization could be also required for coordination with other polarly localized complexes such as adhesins or pili to bring the target membrane closer to the bacterial cell and thus facilitate protein translocation by T6SS.

4.Concluding remarks

Tremendous progress was achieved in understanding the mode of action of T6SS, however, it is clear that there are still many open questions that need to be solved in the future. We need atomic model of the whole assembly; however, since T6SS is both dynamic and regulated, we also need to solve high resolution structures of the individual steps of the assembly process. This will be challenging especially for the membrane complex but also for the transient complexes forming, for example, during sheath-tube copolymerization. Since the live-cell imaging shows that T6SS localization and assembly dynamics can vary significantly between species or under various conditions, more effort will have to be devoted to the accessory proteins unique for certain bacteria. This will certainly reveal novel fascinating mechanisms of dynamic localization of proteins within bacterial cells which will have implications reaching beyond the T6SS field.

Figures

Figure 1. Overview of T6SS assembly and mode of action. (a) T6SS consists of a membrane complex (blue), a baseplate assembled around a central spike (yellow) and a contractile sheath wrapping around a rigid tube (green). The distal end of the sheath is capped (red). Upon activation the membrane complex opens up to allow the passage of spike and tube, baseplate reorients to trigger contraction, and tube is pushed out of the cell by contracting sheath. Contracted sheath is unfolded by ClpV (brown). **(b)** T6SS in prefiring state. Membrane complex: TssJLM in closed state (EMD-xxx, unpublished, 3U66), baseplate: PAAR (4JIV), VgrG (6H3L), TssK, TssF-TssG and TssE (6GIY and 6N38), TssE (6GJ1), Hcp and extended sheath TssB-TssC (5MXN). Sheath-tube complex and the spike are modeled by fitting atomic structures to the EM map of T6SS baseplate of *V. cholerae* (EMD□ 3879). The wedge of T6SS in pre-firing state was modeled by fitting the core bundle of TssF-TssG to T4 phage extended baseplate gp6-gp7 core-bundle (5IV5). Composite structure is superimposed with the subtomogram average of T6SS in *M. xanthus* (EMD-8600). **(c)** Both membrane complex and the baseplate undergo significant reorientation to allow the passage of tube. After contraction, the sheath exposes the surface domain to recruit ClpV (modeled based on ClpB EMD-3776).

Figure 2. Membrane complex structure. (a) TssJ is anchored to the outer membrane by N-terminal acylation. L1-2 loop (red) is required for TssM binding. **(b)** Fifteen copies of TssJ (4Y7O) molecules cap the top of membrane complex, with 3 copies of TssJ top each TssM

pillar. Adjacent TssJ trimers do not make contact for the 5-fold oligomerization. **(c)** TssM dimers oligomerize in the periplasm. Cross-section of the TssM pillars shows the periplasmic gate. 5 pairs of TssM pillars form a narrow central channel with minimal pore size less than 5 Å (yellow arrow). **(d)** TssM anchors to the inner membrane by three N-terminal trans-membrane helices. TssM cytosolic domain is modeled after NTPase-like domain EngB (4DHE) followed by a helical extension modeled after DPY-30 (3G36) as described in (50). The periplasmic domain of TssM carries a putative peptidoglycan-binding motif, modeled after OmpA domain (5U1H), followed by a long helical domain traversing the entire periplasm. The very C-terminus of TssM (red) may extend to extracellular space in native membrane complex. TssM pillar consists of two copies of TssM (blue and gray). Full-length model of TssM is shown for the blue copy. **(e)** Cytosolic domain of TssL (3U66) anchors to the inner membrane by C-terminal transmembrane (TM) helix. The TM helix is responsible for dimerization and the cytosolic domain interacts with both baseplate (red loop interacts with TssE, green loop interacts with TssK) and TssM (central cleft). **(f)** Cryo-EM density of the full trans-envelope complex (EMD-xxx) with TssJ, partial periplasmic domain of TssM fit inside and TssL positioned in the cytoplasmic side of the complex.

Figure 3. Baseplate structure. (a) The T6SS pre-firing baseplate is modeled after the T4 phage baseplate in pre-attachment state (EMD-3374). Both baseplates use a 3-helix "core-bundle" motif for wedge assembly and its attachment to the central hub. T6SS is modeled by matching the $(TssF)_2TssG$ core bundle to $(gp6)_2gp7$ core bundle. **(b)** Atomic structure of T6SS wedge (one TssE and TssG, two TssF and two TssK trimmers). TssK trimers (green and gray) attach to hydrophobic TssG loops (highlighted blue surface). Head domain of TssK (green) is flexible. Two copies of TssF (tan and gray) encircle the TssG (red). The TssE

attaches to the rest of the wedge by interacting with the core bundle (black box), which comprises 3 helices from the N-termini of TssF and TssG.

Figure 4. Structure of the sheath and tube. (a) In extended state (top view, single ring), the sheath protomer (TssB-TssC, blue) contacts the Hcp (gray) with a C-terminal helix (yellow) of TssC. Sheath subunit connection is accomplished by interwoven Domain 1 (green circle). The ClpV binding site (pink) of TssC is tucked inside Domain 3 (light green circle) on the sheath surface. **(b)** Upon contraction, the sheath protomer rotates and detaches from the Hcp tube (top view, single ring). The ClpV binding site is exposed for ClpV docking (brown). In some T6SS, N-terminus of TssB (red) engages TagJ (yellow) to facilitate ClpV association. Scale bar 50 Å. **(c)** and **(d)** the side views of three rings of sheath in extended and contracted state. **(e)** Two rings of Hcp with one sheath protomer. The unstructured loops (residue 50-63, 129-139) and C-terminus (166-172) (dark green) become ordered once they stack into functional tube. One Hcp is colored yellow to show the helical packing. The Domain 3 (black circle) of the extended sheath shields the ClpV binding site of TssC. **(f)** Structure of ClpV N-terminus (3ZRJ) binding to the TssC positioned as the same orientation as in panel (e).

Figure 5. Posttranslational regulation of T6SS activity. Continuous lines – confirmed interactions, dashed lines – predicted interactions. **(a)** In *P. aeruginosa* (purple), membrane damage leads to activation of PpkA by TagQRST and to phosphorylation of Fha. Phosphorylated Fha multimerizes and promotes T6SS assembly. PppA dephosphorylates Fha and stops T6SS assembly. TagF represses T6SS activity independently of TPP by interacting with Fha. **(b)** In *S. marcescens* (yellow), PpkA interacts with RtkS and subsequently phosphorylates Fha, which multimerizes and activates T6SS assembly. PppA dephosphorylates Fha and thus blocks T6SS activity. TagF blocks T6SS activity likely by

468 acting on the membrane complex. **(c)** In *A. tumefaciens* (green), PpkA phosphorylates TssL,
469 which triggers a conformational change in TssM and ATP hydrolysis. Binding of Fha to
470 phosphorylated TssL induces T6SS activity. TagF-PppA blocks T6SS activity by interaction
471 with Fha.

472

473 **Movie 1** – Animation of assembly of T6SS membrane complex, baseplate and sheath-tube
474 complex followed by sheath contraction and tube-spike secretion.

475

476

477 **References:**

478 1. Alcoforado Diniz J, Liu Y, Coulthurst SJ. 2015. Molecular weaponry: diverse effectors
479 delivered by the Type VI secretion system. *Cell. Microbiol.* 17(12):1742–51
480 2. Arisaka F, Yap ML, Kanamaru S, Rossmann MG. 2016. Molecular assembly and
481 structure of the bacteriophage T4 tail. *Biophys. Rev.* 8(4):385–96
482 3. Aschtgen M-S, Bernard CS, Bentzmann SD, Lloubès R, Cascales E. 2008. SciN Is an
483 Outer Membrane Lipoprotein Required for Type VI Secretion in Enteroaggregative
484 Escherichia coli. *J. Bacteriol.* 190(22):7523–31
485 4. Aschtgen M-S, Gavioli M, Dessen A, Lloubès R, Cascales E. 2010. The SciZ protein
486 anchors the enteroaggregative Escherichia coli Type VI secretion system to the cell
487 wall. *Mol. Microbiol.* 75(4):886–99
488 5. Basler M, Ho BT, Mekalanos JJ. 2013. Tit-for-tat: Type VI secretion system
489 counterattack during bacterial cell-cell interactions. *Cell*. 152(4):884–94
490 6. Basler M, Mekalanos JJ. 2012. Type 6 secretion dynamics within and between bacterial
491 cells. *Science*. 337(6096):815

7. Basler M, Pilhofer M, Henderson GP, Jensen GJ, Mekalanos JJ. 2012. Type VI secretion requires a dynamic contractile phage tail-like structure. *Nature*. 483(7388):182–86

8. Böck D, Medeiros JM, Tsao H-F, Penz T, Weiss GL, et al. 2017. In situ architecture, function, and evolution of a contractile injection system. *Science*. 357(6352):713–17

9. Bönemann G, Pietrosiuk A, Diemand A, Zentgraf H, Mogk A. 2009. Remodelling of VipA/VipB tubules by ClpV-mediated threading is crucial for type VI protein secretion. *EMBO J.* 28(4):315–25

10. Boyer F, Fichant G, Berthod J, Vandenbrouck Y, Attree I. 2009. Dissecting the bacterial type VI secretion system by a genome wide in silico analysis: what can be learned from available microbial genomic resources? *BMC Genomics*. 10:104

11. Brackmann M, Nazarov S, Wang J, Basler M. 2017. Using Force to Punch Holes: Mechanics of Contractile Nanomachines. *Trends Cell Biol.* 27(9):623–32

12. Brackmann M, Wang J, Basler M. 2018. Type VI secretion system sheath inter□ subunit interactions modulate its contraction. *EMBO Rep.* 19(2):225–33

13. Brodmann M, Dreier RF, Broz P, Basler M. 2017. Francisella requires dynamic type VI secretion system and ClpB to deliver effectors for phagosomal escape. *Nat. Commun.* 8:15853

14. Bröms JE, Sjöstedt A, Lavander M. 2010. The Role of the Francisella Tularensis Pathogenicity Island in Type VI Secretion, Intracellular Survival, and Modulation of Host Cell Signaling. *Front. Microbiol.* 1:136

15. Carlsson F, Joshi SA, Rangell L, Brown EJ. 2009. Polar localization of virulence-related Esx-1 secretion in mycobacteria. *PLoS Pathog.* 5(1):e1000285

16. Casabona MG, Silverman JM, Sall KM, Boyer F, Couté Y, et al. 2013. An ABC transporter and an outer membrane lipoprotein participate in posttranslational activation of type VI secretion in Pseudomonas aeruginosa. *Environ. Microbiol.* 15(2):471–86

518 17. Cascales E. 2008. The type VI secretion toolkit. *EMBO Rep.* 9(8):735–41
519 18. Chakravortty D, Rohde M, Jäger L, Deiwick J, Hensel M. 2005. Formation of a novel
520 surface structure encoded by Salmonella Pathogenicity Island 2. *EMBO J.*
521 24(11):2043–52
522 19. Chang Y-W, Rettberg LA, Ortega DR, Jensen GJ. 2017. In vivo structures of an intact
523 type VI secretion system revealed by electron cryotomography. *EMBO Rep.*
524 18(7):1090–99
525 20. Charles M, Pérez M, Kobil JH, Goldberg MB. 2001. Polar targeting of Shigella
526 virulence factor IcsA in Enterobacteriacae and Vibrio. *Proc. Natl. Acad. Sci. U. S. A.*
527 98(17):9871–76
528 21. Chen L, Zou Y, She P, Wu Y. 2015. Composition, function, and regulation of T6SS in
529 Pseudomonas aeruginosa. *Microbiol. Res.* 172:19–25
530 22. Cherrak Y, Rapisarda C, Pellarin R, Bouvier G, Bardiaux B, et al. 2018. Biogenesis and
531 structure of a type VI secretion baseplate. *Nat. Microbiol.* 3(12):1404–16
532 23. Cianfanelli FR, Alcoforado Diniz J, Guo M, De Cesare V, Trost M, Coulthurst SJ.
533 2016. VgrG and PAAR Proteins Define Distinct Versions of a Functional Type VI
534 Secretion System. *PLoS Pathog.* 12(6):e1005735
535 24. Clemens DL, Ge P, Lee B-Y, Horwitz MA, Zhou ZH. 2015. Atomic structure of T6SS
536 reveals interlaced array essential to function. *Cell*. 160(5):940–51
537 25. Deville C, Carroni M, Franke KB, Topf M, Bukau B, et al. 2017. Structural pathway of
538 regulated substrate transfer and threading through an Hsp100 disaggregase. *Sci. Adv.*
539 3(8):e1701726
540 26. Dik DA, Marous DR, Fisher JF, Mobashery S. 2017. Lytic transglycosylases:
541 concinnity in concision of the bacterial cell wall. *Crit. Rev. Biochem. Mol. Biol.*
542 52(5):503–42

27. Dix SR, Owen HJ, Sun R, Ahmad A, Shastri S, et al. 2018. Structural insights into the function of type VI secretion system TssA subunits. *Nat Commun*. 9(1):4765

28. Durand E, Nguyen VS, Zoued A, Logger L, Péhau-Arnaudet G, et al. 2015. Biogenesis and structure of a type VI secretion membrane core complex. *Nature*. 523(7562):555–60

29. Durand E, Zoued A, Spinelli S, Watson PJH, Aschtgen M-S, et al. 2012. Structural characterization and oligomerization of the TssL protein, a component shared by bacterial type VI and type IVb secretion systems. *J. Biol. Chem.* 287(17):14157–68

30. Felisberto-Rodrigues C, Durand E, Aschtgen M-S, Blangy S, Ortiz-Lombardia M, et al. 2011. Towards a Structural Comprehension of Bacterial Type VI Secretion Systems: Characterization of the TssJ-TssM Complex of an Escherichia coli Pathovar. *PLOS Pathog.* 7(11):e1002386

31. Förster A, Planamente S, Manoli E, Lossi NS, Freemont PS, Filloux A. 2014. Coevolution of the ATPase ClpV, the sheath proteins TssB and TssC, and the accessory protein TagJ/HsiE1 distinguishes type VI secretion classes. *J. Biol. Chem.* 289(47):33032–43

32. Fritsch MJ, Trunk K, Diniz JA, Guo M, Trost M, Coulthurst SJ. 2013. Proteomic Identification of Novel Secreted Antibacterial Toxins of the Serratia marcescens Type VI Secretion System. *Mol. Cell. Proteomics MCP*. 12(10):2735–49

33. Gates SN, Yokom AL, Lin J, Jackrel ME, Rizo AN, et al. 2017. Ratchet-like polypeptide translocation mechanism of the AAA+ disaggregase Hsp104. *Science*. 357(6348):273–79

34. Geiger T, Pazos M, Lara-Tejero M, Vollmer W, Galán JE. 2018. Peptidoglycan editing by a specific LD-transpeptidase controls the muramidase-dependent secretion of typhoid toxin. *Nat. Microbiol.* 3(11):1243–54

568 35. Gerc AJ, Diepold A, Trunk K, Porter M, Rickman C, et al. 2015. Visualization of the
569 Serratia Type VI Secretion System Reveals Unprovoked Attacks and Dynamic
570 Assembly. *Cell Rep.* 12(12):2131–42
571 36. Ho BT, Basler M, Mekalanos JJ. 2013. Type 6 Secretion System-Mediated Immunity
572 to Type 4 Secretion System-Mediated Horizontal Gene Transfer. *Science*.
573 342(6155):250–53
574 37. Ho BT, Dong TG, Mekalanos JJ. 2014. A view to a kill: the bacterial type VI secretion
575 system. *Cell Host Microbe*. 15(1):9–21
576 38. Hsu F, Schwarz S, Mougous JD. 2009. TagR Promotes PpkA-Catalyzed Type VI
577 Secretion Activation in Pseudomonas aeruginosa. *Mol. Microbiol.* 72(5):1111–25
578 39. Jain S, van Ulsen P, Benz I, Schmidt MA, Fernandez R, et al. 2006. Polar localization
579 of the autotransporter family of large bacterial virulence proteins. *J. Bacteriol.*
580 188(13):4841–50
581 40. Jeong KC, Ghosal D, Chang Y-W, Jensen GJ, Vogel JP. 2017. Polar delivery of
582 Legionella type IV secretion system substrates is essential for virulence. *Proc. Natl.*
583 *Acad. Sci. U. S. A.* 114(30):8077–82
584 41. Joshi A, Kostiuk B, Rogers A, Teschler J, Pukatzki S, Yildiz FH. Rules of
585 Engagement: The Type VI Secretion System in Vibrio cholerae. *Trends Microbiol.*
586 42. Kudryashev M, Wang RY-R, Brackmann M, Scherer S, Maier T, et al. 2015. Structure
587 of the Type VI Secretion System Contractile Sheath. *Cell*. 160(5):952–62
588 43. Laloux G, Jacobs-Wagner C. 2014. How do bacteria localize proteins to the cell pole?
589 *J. Cell Sci.* 127(Pt 1):11–19
590 44. Leiman PG, Basler M, Ramagopal UA, Bonanno JB, Sauder JM, et al. 2009. Type VI
591 secretion apparatus and phage tail-associated protein complexes share a common
592 evolutionary origin. *Proc. Natl. Acad. Sci. U. S. A.* 106(11):4154–59

45. Leiman PG, Shneider MM. 2012. Contractile tail machines of bacteriophages. *Adv. Exp. Med. Biol.* 726:93–114

46. Leung KY, Siame BA, Snowball H, Mok Y-K. 2011. Type VI secretion regulation: crosstalk and intracellular communication. *Host–microbe Interact.* 14(1):9–15

47. Lien Y-W, Lai E-M. 2017. Type VI Secretion Effectors: Methodologies and Biology. *Front. Cell. Infect. Microbiol.* 7:

48. Lin J-S, Pissaridou P, Wu H-H, Tsai M-D, Filloux A, Lai E-M. 2018. TagF-mediated repression of bacterial type VI secretion systems involves a direct interaction with the cytoplasmic protein Fha. *J. Biol. Chem.*

49. Lin J-S, Wu H-H, Hsu P-H, Ma L-S, Pang Y-Y, et al. 2014. Fha Interaction with Phosphothreonine of TssL Activates Type VI Secretion in Agrobacterium tumefaciens. *PLoS Pathog.* 10(3):e1003991

50. Logger L, Aschtgen M-S, Guérin M, Cascales E, Durand E. 2016. Molecular Dissection of the Interface between the Type VI Secretion TssM Cytoplasmic Domain and the TssG Baseplate Component. *J. Mol. Biol.* 428(22):4424–37

51. Lossi NS, Manoli E, Simpson P, Jones C, Hui K, et al. 2012. The archetype Pseudomonas aeruginosa proteins TssB and TagJ form a novel subcomplex in the bacterial type VI secretion system. *Mol. Microbiol.* 86(2):437–56

52. Ma L-S, Lin J-S, Lai E-M. 2009. An IcmF family protein, ImpLM, is an integral inner membrane protein interacting with ImpKL, and its walker a motif is required for type VI secretion system-mediated Hcp secretion in Agrobacterium tumefaciens. *J. Bacteriol.* 191(13):4316–29

53. Ma L-S, Narberhaus F, Lai E-M. 2012. IcmF Family Protein TssM Exhibits ATPase Activity and Energizes Type VI Secretion. *J. Biol. Chem.* 287(19):15610–21

54. Miyata ST, Bachmann V, Pukatzki S. 2013. Type VI secretion system regulation as a consequence of evolutionary pressure. *J. Med. Microbiol.* 62(Pt_5):663–76

619 55. Morgan JK, Luedtke BE, Shaw EI. 2010. Polar localization of the Coxiella burnetii
620 type IVB secretion system. *FEMS Microbiol. Lett.* 305(2):177–83
621 56. Motley ST, Lory S. 1999. Functional characterization of a serine/threonine protein
622 kinase of Pseudomonas aeruginosa. *Infect. Immun.* 67(10):5386–94
623 57. Mougous JD, Gifford CA, Ramsdell TL, Mekalanos JJ. 2007. Threonine
624 phosphorylation post-translationally regulates protein secretion in Pseudomonas
625 aeruginosa. *Nat Cell Biol*. 9(7):797–803
626 58. Narita S, Tokuda H. 2006. An ABC transporter mediating the membrane detachment of
627 bacterial lipoproteins depending on their sorting signals. *FEBS Lett.* 580(4):1164–70
628 59. Nazarov S, Schneider JP, Brackmann M, Goldie KN, Stahlberg H, Basler M. 2018.
629 Cryo-EM reconstruction of Type VI secretion system baseplate and sheath distal end.
630 *EMBO J.* 37(4):
631 60. Nguyen VS, Logger L, Spinelli S, Legrand P, Huyen Pham TT, et al. 2017. Type VI
632 secretion TssK baseplate protein exhibits structural similarity with phage receptor-
633 binding proteins and evolved to bind the membrane complex. *Nat. Microbiol.*
634 2(9):17103
635 61. Ostrowski A, Cianfanelli FR, Porter M, Mariano G, Peltier J, et al. 2018. Killing with
636 proficiency: Integrated post-translational regulation of an offensive Type VI secretion
637 system. *PLoS Pathog.* 14(7):e1007230
638 62. Park Y-J, Lacourse KD, Cambillau C, DiMaio F, Mougous JD, Veesler D. 2018.
639 Structure of the type VI secretion system TssK–TssF–TssG baseplate subcomplex
640 revealed by cryo-electron microscopy. *Nat. Commun.* 9(1):5385
641 63. Pietrosiuk A, Lenherr ED, Falk S, Bönemann G, Kopp J, et al. 2011. Molecular Basis
642 for the Unique Role of the AAA+ Chaperone ClpV in Type VI Protein Secretion. *J.*
643 *Biol. Chem.* 286(34):30010–21

644 64. Planamente S, Salih O, Manoli E, Albesa□Jové D, Freemont PS, Filloux A. 2016.
645 TssA forms a gp6□like ring attached to the type VI secretion sheath. *EMBO J.*
646 35(15):1613–27
647 65. Pukatzki S, Ma AT, Revel AT, Sturtevant D, Mekalanos JJ. 2007. Type VI secretion
648 system translocates a phage tail spike-like protein into target cells where it cross-links
649 actin. *Proc. Natl. Acad. Sci. U. S. A.* 104(39):15508–13
650 66. Pukatzki S, Ma AT, Sturtevant D, Krastins B, Sarracino D, et al. 2006. Identification of
651 a conserved bacterial protein secretion system in Vibrio cholerae using the
652 Dictyostelium host model system. *Proc Natl Acad Sci U A*. 103(5):1528–33
653 67. Quentin D, Ahmad S, Shanthamoorthy P, Mougous JD, Whitney JC, Raunser S. 2018.
654 Mechanism of loading and translocation of type VI secretion system effector Tse6. *Nat*
655 *Microbiol*. 3(10):1142–52
656 68. Rao VA, Shepherd SM, English G, Coulthurst SJ, Hunter WN. 2011. The structure of
657 Serratia marcescens Lip, a membrane-bound component of the type VI secretion
658 system. *Acta Crystallogr. D Biol. Crystallogr.* 67(12):1065–72
659 69. Rapisarda C, Cherrak Y, Kooger R, Schmidt V, Pellarin R, et al. 2018. In situ and high-
660 resolution Cryo-EM structure of the Type VI secretion membrane complex. *bioRxiv*, p.
661 441683
662 70. Ringel PD, Hu D, Basler M. 2017. The Role of Type VI Secretion System Effectors in
663 Target Cell Lysis and Subsequent Horizontal Gene Transfer. *Cell Rep.* 21(13):3927–40
664 71. Robb CS, Nano FE, Boraston AB. 2010. Cloning, expression, purification,
665 crystallization and preliminary X-ray diffraction analysis of intracellular growth locus
666 E (IglE) protein from Francisella tularensis subsp. novicida. *Acta Crystallograph. Sect.*
667 *F Struct. Biol. Cryst. Commun.* 66(12):1596–98
668 72. Rosch J, Caparon M. 2004. A microdomain for protein secretion in Gram-positive
669 bacteria. *Science*. 304(5676):1513–15

670 73. Salih O, He S, Planamente S, Stach L, MacDonald JT, et al. 2018. Atomic Structure of
671 Type VI Contractile Sheath from Pseudomonas aeruginosa. *Structure*. 26(2):329-336
672 e3
673 74. Santin YG, Cascales E. 2017. Domestication of a housekeeping transglycosylase for
674 assembly of a Type VI secretion system. *EMBO Rep.* 18(1):138–49
675 75. Santin YG, Doan T, Lebrun R, Espinosa L, Journet L, Cascales E. 2018. In vivo TssA
676 proximity labelling during type VI secretion biogenesis reveals TagA as a protein that
677 stops and holds the sheath. *Nat. Microbiol.* 3(11):1304
678 76. Scheurwater EM, Burrows LL. 2011. Maintaining network security: how
679 macromolecular structures cross the peptidoglycan layer. *FEMS Microbiol. Lett.*
680 318(1):1–9
681 77. Schwarz S, Singh P, Robertson JD, LeRoux M, Skerrett SJ, et al. 2014. VgrG-5 is a
682 Burkholderia type VI secretion system-exported protein required for multinucleated
683 giant cell formation and virulence. *Infect. Immun.* 82(4):1445–52
684 78. Schwarz S, West TE, Boyer F, Chiang W-C, Carl MA, et al. 2010. Burkholderia type
685 VI secretion systems have distinct roles in eukaryotic and bacterial cell interactions.
686 *PLoS Pathog.* 6(8):e1001068
687 79. Sciara G, Bebeacua C, Bron P, Tremblay D, Ortiz-Lombardia M, et al. 2010. Structure
688 of lactococcal phage p2 baseplate and its mechanism of activation. *Proc. Natl. Acad.*
689 *Sci. U. S. A.* 107(15):6852–57
690 80. Scott ME, Dossani ZY, Sandkvist M. 2001. Directed polar secretion of protease from
691 single cells of Vibrio cholerae via the type II secretion pathway. *Proc. Natl. Acad. Sci.*
692 *U. S. A.* 98(24):13978–83
693 81. Shneider MM, Buth SA, Ho BT, Basler M, Mekalanos JJ, Leiman PG. 2013. PAAR-
694 repeat proteins sharpen and diversify the type VI secretion system spike. *Nature*.
695 500(7462):350–53

696 82. Silverman JM, Austin LS, Hsu F, Hicks KG, Hood RD, Mougous JD. 2011. Separate
697 inputs modulate phosphorylation-dependent and -independent type VI secretion
698 activation. *Mol. Microbiol.* 82(5):1277–90
699 83. Spínola-Amilibia M, Davó-Siguero I, Ruiz FM, Santillana E, Medrano FJ, Romero A.
700 2016. The structure of VgrG1 from Pseudomonas aeruginosa, the needle tip of the
701 bacterial type VI secretion system. *Acta Crystallogr. Sect. Struct. Biol.* 72(Pt 1):22–33
702 84. Taylor NMI, Prokhorov NS, Guerrero-Ferreira RC, Shneider MM, Browning C, et al.
703 2016. Structure of the T4 baseplate and its function in triggering sheath contraction.
704 *Nature*. 533(7603):346
705 85. Typas A, Banzhaf M, Gross CA, Vollmer W. 2011. From the regulation of
706 peptidoglycan synthesis to bacterial growth and morphology. *Nat. Rev. Microbiol.*
707 10(2):123–36
708 86. Veesler D, Spinelli S, Mahony J, Lichière J, Blangy S, et al. 2012. Structure of the
709 phage TP901-1 1.8 MDa baseplate suggests an alternative host adhesion mechanism.
710 *Proc. Natl. Acad. Sci. U. S. A.* 109(23):8954–58
711 87. Vettiger A, Basler M. 2016. Type VI Secretion System Substrates Are Transferred and
712 Reused among Sister Cells. *Cell*. 167(1):99-110.e12
713 88. Vettiger A, Winter J, Lin L, Basler M. 2017. The type VI secretion system sheath
714 assembles at the end distal from the membrane anchor. *Nat. Commun.* 8:16088
715 89. Wang J, Brackmann M, Castaño-Díez D, Kudryashev M, Goldie KN, et al. 2017. Cryo-
716 EM structure of the extended type VI secretion system sheath-tube complex. *Nat.*
717 *Microbiol.* 2(11):1507–12
718 90. Weber BS, Hennon SW, Wright MS, Scott NE, de Berardinis V, et al. 2016. Genetic
719 Dissection of the Type VI Secretion System in Acinetobacter and Identification of a
720 Novel Peptidoglycan Hydrolase, TagX, Required for Its Biogenesis. *mBio*. 7(5):

721 91. Wilton M, Wong MJQ, Tang L, Liang X, Moore R, et al. 2016. Chelation of
722 Membrane-Bound Cations by Extracellular DNA Activates the Type VI Secretion
723 System in Pseudomonas aeruginosa. *Infect. Immun.* 84(8):2355–61
724 92. Yang Z, Zhou X, Ma Y, Zhou M, Waldor MK, et al. 2018. Serine/threonine kinase
725 PpkA coordinates the interplay between T6SS2 activation and quorum sensing in the
726 marine pathogen Vibrio alginolyticus. *Environ. Microbiol.*
727 93. Yin M, Yan Z, Li X. 2019. Architecture of type VI secretion system membrane core
728 complex. *Cell Res.*, p. 1
729 94. Yu H, Lupoli TJ, Kovach A, Meng X, Zhao G, et al. 2018. ATP hydrolysis-coupled
730 peptide translocation mechanism of Mycobacterium tuberculosis ClpB. *Proc. Natl.*
731 *Acad. Sci.* 115(41):E9560–69
732 95. Zheng J, Ho B, Mekalanos JJ. 2011. Genetic analysis of anti-amoebae and anti-
733 bacterial activities of the type VI secretion system in Vibrio cholerae. *PloS One*.
734 6(8):e23876
735 96. Zheng J, Leung KY. 2007. Dissection of a type VI secretion system in Edwardsiella
736 tarda. *Mol. Microbiol.* 66(5):1192–1206
737 97. Zoued A, Cassaro CJ, Durand E, Douzi B, España AP, et al. 2016. Structure–Function
738 Analysis of the TssL Cytoplasmic Domain Reveals a New Interaction between the
739 Type VI Secretion Baseplate and Membrane Complexes. *J. Mol. Biol.* 428(22):4413–
740 23
741 98. Zoued A, Duneau J-P, Durand E, España AP, Journet L, et al. 2018. Tryptophan-
742 mediated Dimerization of the TssL Transmembrane Anchor Is Required for Type VI
743 Secretion System Activity. *J. Mol. Biol.* 430(7):987–1003
744 99. Zoued A, Durand E, Bebeacua C, Brunet YR, Douzi B, et al. 2013. TssK Is a Trimeric
745 Cytoplasmic Protein Interacting with Components of Both Phage-like and Membrane

Anchoring Complexes of the Type VI Secretion System. *J. Biol. Chem.* 288(38):27031–41

100. Zoued A, Durand E, Brunet YR, Spinelli S, Douzi B, et al. 2016. Priming and polymerization of a bacterial contractile tail structure. *Nature*. 531(7592):59–63

101. Zoued A, Durand E, Santin YG, Journet L, Roussel A, et al. 2017. TssA: The cap protein of the Type VI secretion system tail. *BioEssays*. 39(10):1600262

Figures.

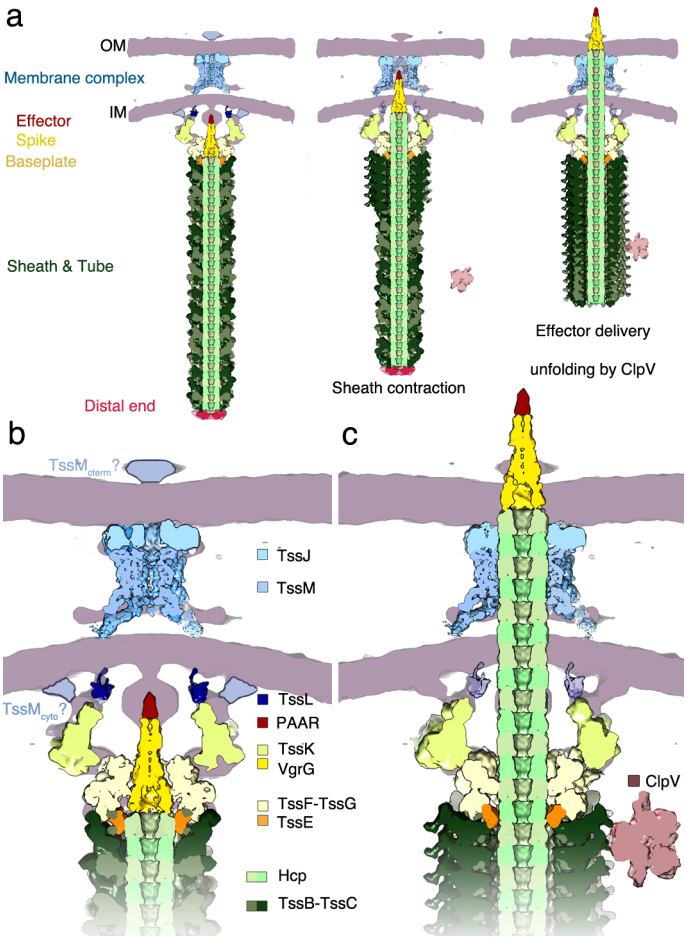

Figure 1.

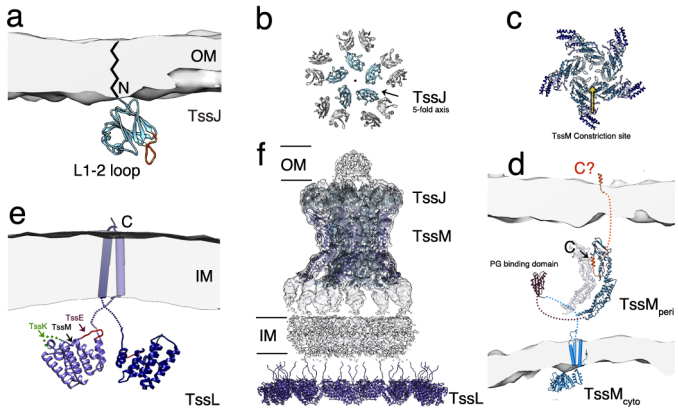

757

758 Figure 2.

759

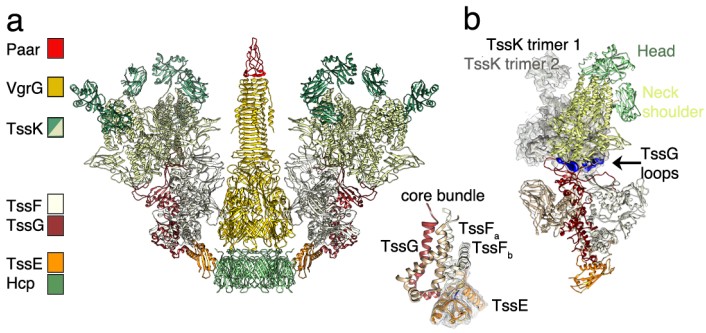

760

761 Figure 3.

762

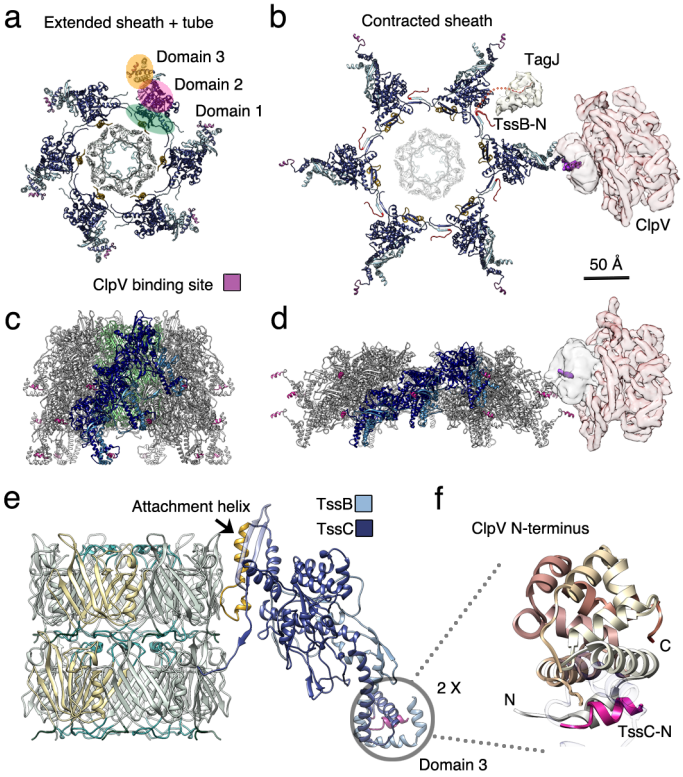

763

764 Figure 4.